

Filtering of bottom sources through the ocean.

G. Pedersen

Department of Mathematics, University of Oslo, PO box 1053, 0316 Oslo, Norway

April 29, 2011

Abstract

This report sketches the use of the Green function from Kajiura (1963) [1].

1 Introduction

Simulations of tsunamis from earthquakes are generally start from an initial elevation of the sea surface. To this end, the vertical uplift of the sea-bed is generally copied onto the sea surface, which may lead to sharp and unphysical gradients. When the rupture reach all the way to crust surface, there is, in principle, even a discontinuity in the uplift of the sea-bed. For a long and wide ruptures this may be removed as described in [3, 4]. The method may be generalized to all forms of plane distributions. However, to capture three-dimensional features it is necessary to apply the full Green function.

The procedure described below is based on an assumption of instantaneous bottom deformation. A true earthquake is a complicated process with a finite time story and compression waves in the water. Hence, the procedure will mainly remove unphysically short scales, but not reproduce the tsunami generation process in detail. Submarine slides require anyhow a source representation of finite extent in time and space, which may be represented numerically as a sequence of bottom sources. The filter may then be applied to each field in such a sequence.

2 The Green function

From the excellent reference [1] we adopt the Green function for the point source in unitary depth

$$G(r) = \frac{1}{2\pi} \int_0^\infty \frac{m J_0(mr)}{\cosh m} dm, \quad (1)$$

Where r is the distance from the point. Expansion of the reciprocal of the hyperbolic cosine in exponentials yields the series

$$G(r) = R(r^2) = \frac{1}{\pi} \sum_{n=0}^{\infty} \frac{(-1)^n (2n+1)}{\{(2n+1)^2 + r^2\}^{\frac{3}{2}}}. \quad (2)$$

The result for different values of N_L is shown in figure 1. A measure of the quality of G is the volume

$$V = 2\pi \int_0^\infty r G(r) dr,$$

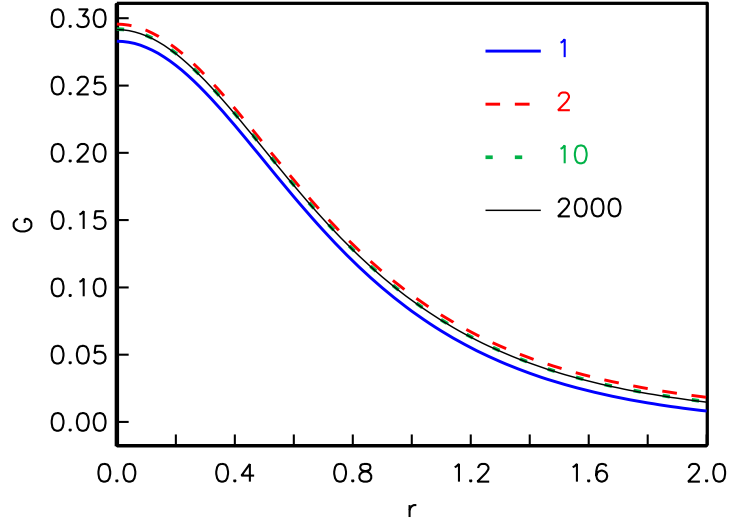


Figure 1: G as function of r for different values of N_L .

which should equal unity. We find

N_L	1	2	5	10	200	2000
V	0.38	1.48	0.77	1.09	1.00034	1.00003

The large deviation of V in comparison to figure 1 is due to moderate errors for large r which become accentuated through the integration. Generally, the value $N_L = 2000$ is recommended.

The function $R(s)$ is tabulated on the interval $0 \leq s \leq B^2$ with increment Δs . The Value of G for any value of s is then obtained by either linear interpolation or interpolation by cubic splines. From figure 2 we see that B may be chosen as 5, which is used subsequently, or larger.

In depth h the the response to a source distribution $D(\mathbf{r})$ may be approximated by

$$\eta(\mathbf{r}) = h^{-2} \iint_{|\mathbf{r}-\mathbf{r}'| \leq B} R((\mathbf{r}-\mathbf{r}')^2) D(\mathbf{r}') dx' dy'. \quad (3)$$

3 Numerical representation of bottom sources

The source distribution $D(x, y)$ is discretized on a grid $\mathbf{r}_{ij} = (x_i, y_j)$ by allotting a point source of strength

$$\sigma \Delta x \Delta y D_{ij},$$

to each grid point. Here h is the water depth and σ is a correction factor, which is defined below. The response from such a source then becomes

$$H_{ij}(\mathbf{r}) = \sigma \frac{\Delta x \Delta y}{h^2} D_{ij} R(|\mathbf{r} - \mathbf{r}_{ij}|^2 / h^2), \quad (4)$$

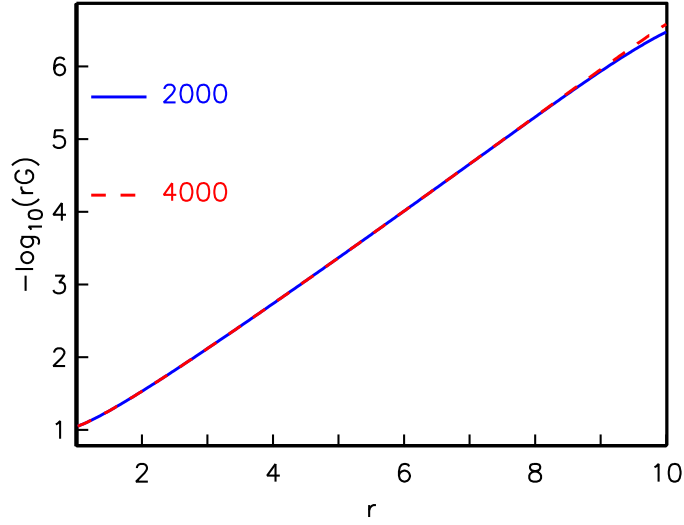


Figure 2: The Brigg logarithm of rG as function of r for two values of N_L .

When R is tabulated, as described above, interpolation then gives the contribution from this to another point $\mathbf{r}_{k\ell}$ as

$$H_{ij}(\mathbf{r}_{k\ell}) = \sigma \frac{\Delta x \Delta y}{h^2} D_{ij} R_{k-i, \ell-j}, \quad (5)$$

where

$$R_{n,m} = R \left(\frac{(n\Delta x)^2 + (m\Delta y)^2}{h^2} \right). \quad (6)$$

The indexed quantity $R_{n,m}$ may be invoked as a an array of finite, and generally even of moderate, size. All entries where $n\Delta x$ and $m\Delta y$ are larger than the truncation limit (see preceding section), B , may be omitted. We denote the limitations n_x and n_y , such that $-n_x \leq n \leq n_x$ and $-n_y \leq m \leq n_y$. naturally, $R_{n,m}$ possess the symmetries

$$R_{\pm n, \pm m} = R_{n,m}.$$

In principle (4) and (5) are only valid in constant depth. However, they are good approximations as long as the depth changes slowly in the sense $|\nabla h|B \ll h$. In general, a specific $R_{n,m}$ must be interpolated from the table for each grid point. If constant depth may be assumed, at least as a first approximation¹, this local array may be computed only once.

The total response is found simply by assembling the contributions from all the point sources

$$\eta_{k\ell} = \sum_i \sum_j H_{ij}(\mathbf{r}_{k\ell}), \quad (7)$$

which, save for the factor σ , corresponds to the midpoint rule applied to (3).

¹This is not an unnatural assumption since the most important effect of the procedure is to remove unphysically short wavelengths.

We define the discrete “volume” of the source by summation over the whole grid

$$\sum_{i,j} D_{ij} \Delta x \Delta y,$$

corresponding to a mid-point integration rule. To preserve the part of this volume, associated with each points source, exactly during the response we must require

$$1 = \sigma \frac{\Delta x \Delta y}{h^2} \sum_{n=-n_x}^{n_x} \sum_{m=-n_y}^{n_y} R_{n,m}, \quad (8)$$

which determine the factor σ . The factor σ mainly depends on $\Delta x/h$ and $\Delta y/h$ and to a smaller extent on Δs (increment in tabulated Green function), N_L (number of terms in series for Green function) and B . When $\Delta x = \Delta y$ we find the values

$\Delta x/h$	0.1	0.2	0.5	1	3
σ	1.0009	1.0008	1.0006	0.9846	0.3668

We see that σ stays close to unity until Δx becomes larger than h . In this case the grid cannot resolve the effects of the filtering in the sea surface response properly. Moreover, the main contribution to the double sum in (8) then stems from $R_{0,0}$ and we are close to copy the source onto the surface, as must be done for very coarse grids.

4 Tests and examples

4.1 The response of a plane source

A simple, plane unitary source, in unitary depth, is defined by

$$D(x, y) = e^{-\frac{x^2}{L^2}}, \quad (9)$$

such that L is a measure of the source width. To avoid 3D effects in the mid part of the computational domain the length of the source must be larger than $B = 5$. A span $-4L < y < 4L$ has been employed. The surface response is computed in the present 3D fashion as well as by the use of plane point sources described in [3]. Independent implementation of the plane point sources, together with piecewise constant and linear source distributions, were made during the work on [2]. Transects along $y = 0$ is depicted in figure 3. We observe that the two response models coincide closely and that the surface response differ markedly from the bottom source distribution for $L = 2$ and $L = 5$, but not for $L = 10$.

4.2 The response of a cone

A simple, smooth and confined source is defined as

$$D(x, y) = e^{-\frac{x^2+y^2}{L^2}}. \quad (10)$$

Again L is a measure of the source extent and the computational domain is defined by $-4L < x < 4L$ and $-4L < y < 4L$. Transects along $y = 0$ is depicted in figure 4. Comparing with figure 3 we observe that a larger reduction of the response for the smaller L , as should be expected. Moreover, the response is well computed for $\Delta x = h$. Provided the computational domain is increased sufficiently, the relative volume change between the total source and response is observed to fall below 10^{-10} in a double precision run.

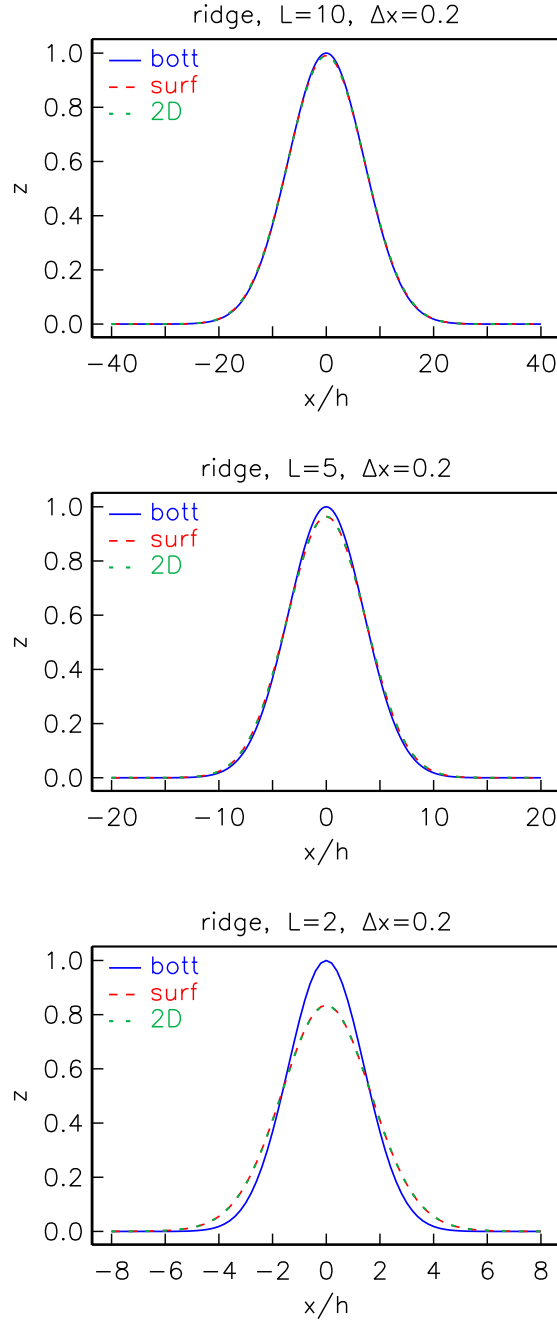


Figure 3: The surface response for a plane source. The present and 2D-computation is marked by *surf* and *3D* respectively.

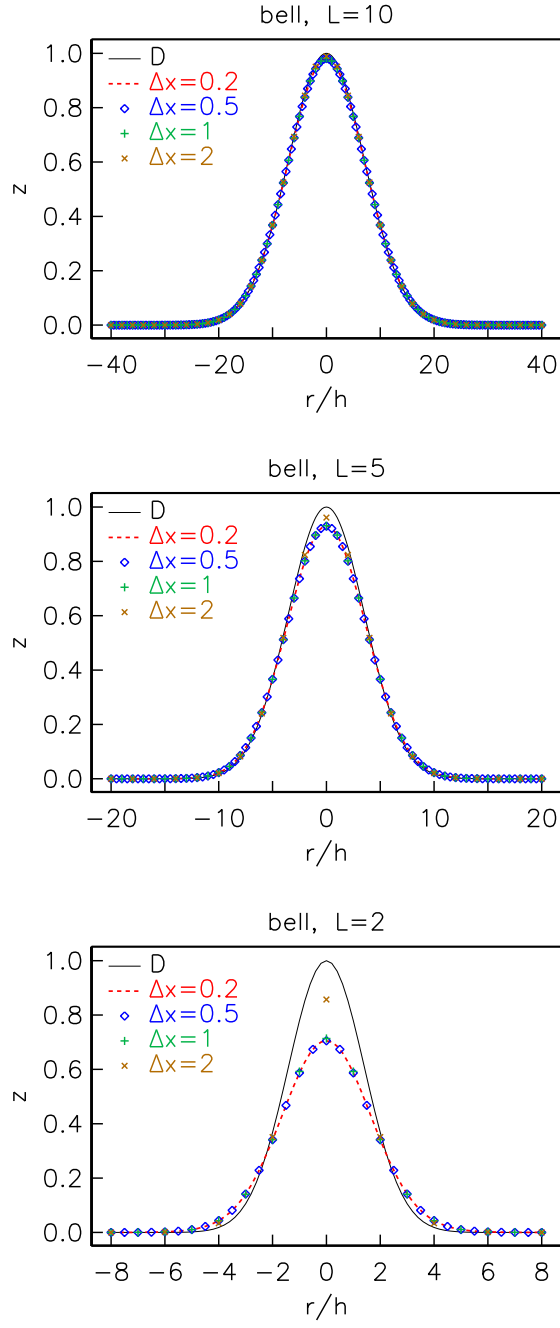


Figure 4: The surface response for a conical source. Different choices for $\Delta x/h$ are included.

4.3 An Okada type source

Okada's method is used to produce a sea bed uplift for a failure of length 140km, width 50km, a dip angle of 12° and a slip of 8m. The ocean depth is set to 5km and the grid increment is 2km, in both directions. The orientation of the fault is at 45° angle relative to the axes. The source and the response are shown in the upper two panels of figure 5. In the lower panel a transect is presented where also the matched asymptotic solution from [3] is included. The asymptotic solution is designed to remove the unphysical discontinuity; and work well to that end. On the other hand, other short features, which are not linked to the plate boundary surface are not modified in this solution. Hence, the deviation from the full response at the depression.

References

- [1] A. Kajiura. The leading wave of a tsunami. *Bulletin of the Earthquake Research Institute*, 41:535–571, 1963.
- [2] F. Løvholt, G. Pedersen, D. Kühn S. Bazin, R. E. Bredesen, H. Bungum, and C. Harbitz. Stochastic analysis of tsunami run-up due to heterogeneous co-seismic slip. 2011. In progress.
- [3] G. Pedersen. A note on tsunami generation by earthquakes. Preprint Series in Applied Mathematics 4, Dept. of Mathematics, University of Oslo, Norway, 2001.
- [4] F. Løvholt, H. Bungum, C.B. Harbitz, S. Glimsdal, C. D. Lindholm, and G. Pedersen. Earthquake related tsunami hazard along the western coast of Thailand. *Natural hazards and earth system sciences*, 6:1–18, 2006.

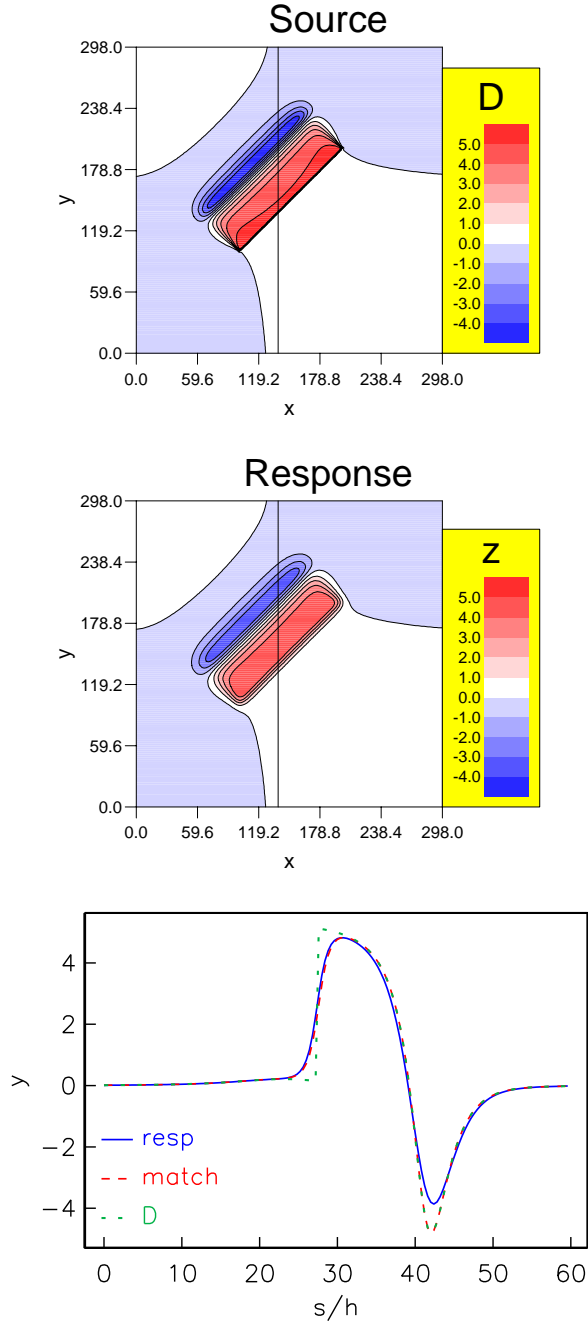


Figure 5: The surface responses to an earthquake source. Lower panel: a transect, as indicated on the upper panels. *resp*, *match* and *D* denotes the response, the source and the result obtained by asymptotic matching, respectively.